Chemical Physics Letters 645 (2016) 88–91

Contents lists available at ScienceDirect

Chemical Physics Letters

journal homepage: www.elsevier.com/locate/cplett

Reaction kinetics of the CN radical with methyl bromide

Michael Hodny, John F. Hershberger*

Department of Chemistry and Biochemistry, North Dakota State University, Dept. 2735, PO Box 6050, Fargo, ND 58108-6050, United States

ARTICLE INFO

Article history:
Received 6 November 2015
In final form 16 December 2015
Available online 24 December 2015

ABSTRACT

The kinetics of the $CN + CH_3Br$ reaction were studied using transient infrared laser absorption spectroscopy to detect CN reactants and HCN products. This reaction has a rate constant of $k = (2.20 \pm 0.6) \times 10^{-12} \exp(453 \pm 98/T)\,cm^3\,molecule^{-1}\,s^{-1}$ over the range 298–523 K. Hydrogen abstraction to produce $HCN + CH_2Br$ is only a minor reaction product, with a branching fraction of 0.12 ± 0.02. Other product channels, including $BrCN + CH_3$, $CH_2CN + HBr$, $CH_3CN + Br$ are likely. An upper limit of 0.01 was established for the HBr yield. These results are in qualitative agreement with recent ab initio calculations.

1. Introduction

The kinetics of the CN radical are of interest due to the role of this molecule in combustion chemistry and atmospheric chemistry. Previous kinetic studies of CN reactions include measurements with a variety of molecules such as saturated and unsaturated hydrocarbons [1–13], O_2 [1,14–22], NO [21,23], and NO_2 [22,23]. Past work in our laboratory has included study of CN reactions with O_2 [24,25], NO_2 [26], OCS [27], CS_2 [28], SO_2 [28], HCNO [29,30], small primary alcohols [31], and chlorinated methanes including CH_3Cl [32]. To date, however, there is no experimental literature on the kinetics of CN reactions with CH_3Br, methyl bromide. This molecule is a trace component of the atmosphere, partly due to recent use as a fumigant, and plays a role in stratospheric ozone depletion and is a greenhouse gas. There is, however, a recent ab initio study of reactions of CN with several halomethanes, including CH_3Cl and CH_3Br [33]. In that study, reaction pathways were calculated at the G4 level of theory, using B3LYP/GTBas3 and/or QCISD/GTBas3 optimized structures. The most probable reaction channels were found to be either hydrogen abstraction or halogen abstraction by the carbon atom on CN. The lowest energy pathway for the $CN + CH_3Cl$ reaction was the expected hydrogen abstraction to produce $HCN + CH_2Cl$; this prediction is consistent with the experimental observation of a positive activation energy [32], typically observed for hydrogen abstraction reactions. For $CN + CH_3Br$, however, the two reaction pathways were calculated to have nearly identical barrier heights: hydrogen abstraction (4.9 kcal/mole standard Gibbs energy of activation) to produce $HCN + CH_2Br$, and attack at the bromine atom (5.0 kcal/mole standard Gibbs energy of activation) to produce $BrCN + CH_3$, $CH_2CN + HBr$, or $CH_3CN + Br$ [33]. This calculation therefore suggests the possibility that HCN is not necessarily the major product of this reaction. No experimental data has been previously reported on the kinetics of this reaction. The primary goal of the experimental study described here is to test that prediction. We report measurements of total rate constants and quantitative HCN product yields:

$$CN + CH_3Br \rightarrow HCN + CH_2Br \quad \Delta G^\circ = -115.5\,kJ/mol \tag{1a}$$

$$\rightarrow CH_2CN + HBr \quad \Delta G^\circ = -182.0\,kJ/mol \tag{1b}$$

$$\rightarrow CH_3CN + Br \quad \Delta G^\circ = -211.7\,kJ/mol \tag{1c}$$

$$\rightarrow BrCN + CH_3 \tag{1d}$$

The thermodynamic values are obtained from the ab initio study [33]; none was reported for channel (1d).

2. Experimental

Cyanogen iodide (ICN) was photolyzed by 266 nm light from the fourth harmonic of an Nd:YAG laser (Continuum Surelite-II):

$$ICN + h\nu(266\,nm) \rightarrow CN + I$$

CN radicals and HCN reaction products were detected by time-resolved infrared diode laser absorption spectroscopy using lead salt diode lasers (Laser Components) operating at 85–110 K. A 5-cm CaF_2 lens was used to collimate the infrared light, and this beam was combined with the UV light from the Nd:YAG laser by a dichroic mirror. Iris diaphragms were used to restrict both beams to 6 mm diameter, and both beams were passed through a single pass absorption cell (146 cm length for room

* Corresponding author.
E-mail address: john.hershberger@ndsu.edu (J.F. Hershberger).

http://dx.doi.org/10.1016/j.cplett.2015.12.036
0009-2614/

temperature experiments, 143 cm length for elevated temperature measurements). The beams were separated by a monochromator, and the IR beam was focused onto a 1 mm InSb detection chip (Cincinnati Electronics, ~1 μs response time). Transient signals were recorded and signal averaged on a digital oscilloscope, then stored on a computer for analysis. Rate coefficient measurements were obtained over the temperature range 298–523 K. Elevated temperatures were achieved by resistive heating, and temperatures were measured with a thermocouple. Product yield measurements were performed at 298 K. Typical reaction conditions were P(ICN) = 0.1 Torr (3.24×10^{15} molecule cm^{-3}), $P(SF_6)$ = 0.5 Torr (1.62×10^{16} molecule cm^{-3}), and $P(CH_3Br)$ varied over the range 0.0–2.0 Torr (0.0–6.38×10^{16} molecule cm^{-3}), resulting in total pressure of 0.6–2.6 Torr.

Typical photolysis pulse laser energies were 7–12 mJ/pulse. Based on a previously measured 266 nm absorption coefficient for ICN of 0.009 cm^{-1} $Torr^{-1}$ [34], and assuming a unity quantum yield, we estimate typical initial number densities of $[CN]0 \sim 3 \times 10^{13}$ molecules cm^{-3}. Only a negligible increase in temperature is caused by absorption of the UV laser pulse. CH_3Br absorbs only very weakly at 266 nm, [35] so photolytic formation and subsequent secondary chemistry of CH_3 or Br is negligible. Data was collected using static gas fills, as the low vapor pressure of the ICN reagent makes a flow experiment difficult. Each gas fill was limited to 10–20 photolysis laser pulses in order to minimize depletion of precursor molecules or accumulation of product molecules. The SF_6 was present as a nonreactive buffer gas, primarily to promote vibrational and rotational relaxation of reactant and product molecules to a Boltzmann distribution. It's effectiveness at relaxing vibrational excitation has been demonstrated in an early publication from our laboratory [36] for detection of some product molecules, but not HCN; this issue is discussed in Section 3.2.

ICN (Fluka, 97%) was purified by vacuum sublimation to remove any dissolved gasses. CH_3Br (Aldrich) was purified by several freeze-pump-thaw cycles at 77 K.

The following molecules were probed using IR diode laser absorption spectroscopy:

$$CN(v = 1 \rightarrow v = 0) \quad R(10) \quad \text{at} \quad 2081.689\ cm^{-1}$$

$$HCN(v = 1 \leftarrow v = 0) \quad P(19) \quad \text{at} \quad 3251.822\ cm^{-1}$$

The HITRAN database [37] as well as other published spectroscopic data [38,39] was used for locating and identifying spectral lines of HCN. Other published sources were used to locate and identify spectral lines of CN [40] and BrCN [41].

3. Results

3.1. Total rate coefficients

The total rate coefficient of the CN + CH_3Br reaction was determined by direct time-resolved detection of CN radicals, as shown in Figure 1. The rapid rise in absorption is attributed to photolytic formation of CN; the precursor is known to produce primarily ground vibrational state but rotationally hot CN; this rotational excitation is quickly (<10 μs) relaxed to a Boltzmann distribution under our conditions. The slower decay of the transient signal is attributed to loss of CN; in the absence of CH_3Br reagent, this loss includes diffusional loss of CN from the probed reaction volume as well as reaction of CN with trace O_2 (probably the dominant contribution, as vacuum sublimation of ICN crystals removes most but not all dissolved air) and to some extent, radical–radical chemistry such as self reaction. Upon addition of CH_3Br, the decay rate was found to substantially increase, and was well described by a single exponential decay. Figure 2 shows the decay rate as a function

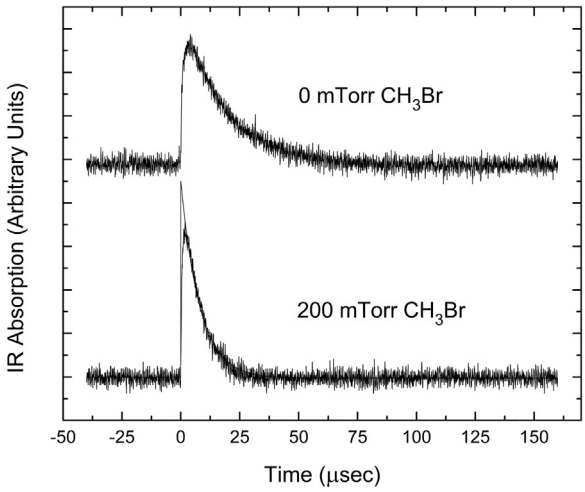

Figure 1. Infrared absorption transients, detecting [CN] vs time. Upper trace: without added reagent. Lower trace: with 0.2 Torr (6.5×10^{15} molecule cm^{-3}) of CH_3Br reagent. Also shown on lower trace is a single exponential decay fit to the data. Other conditions (both traces): P(ICN) = 0.1 Torr, $P(SF_6)$ = 0.5 Torr.

of CH_3Br pressure. Under our conditions, pseudofirst order kinetics, i.e. $[CN] \ll [CH_3Br]$ applies at CH_3Br pressures above ~20 mTorr. Therefore, a standard treatment gives

$$[CN]_t = [CN]_0 \exp(-k't)$$

$$k' = k_1[CH_3Br] + k_0$$

where k' is the observed pseudo-first order CN signal decay, k_1 is the desired bimolecular rate coefficient, and k_0 is the pseudo-first order decay in the absence of methyl bromide reagent (attributed to self-reaction, reaction with trace oxygen, and/or diffusional loss out of the probed beam volume). Figure 2 shows a plot of k' as a function of $[CH_3Br]$. The desired bimolecular rate coefficient k_1 is obtained from the slope of this plot.

Rate coefficients were determined over the temperature range 298–523 K. Figure 3 shows an Arrhenius plot. As is shown, the data show that the total rate constant has only a very modest temperature dependence, varying by only a factor of two over the range of temperatures. This small range in rate constants is the primary reason for the large apparent scatter in Figure 3. A small but definitely negative activation energy is observed. This is typical of addition-elimination or radical–radical reactions rather than direct

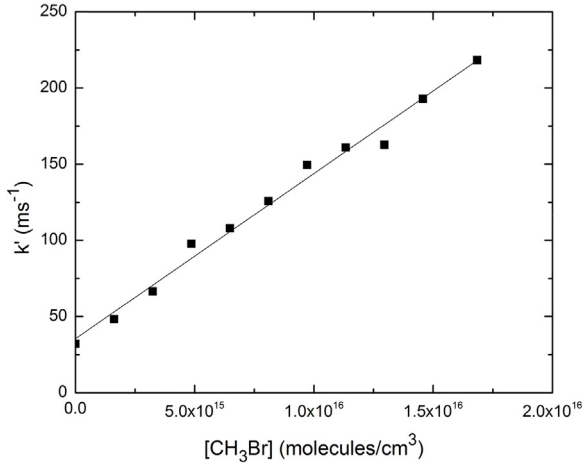

Figure 2. Plot of pseudo-first-order decay rate k' vs. CH_3Br pressure. Data obtained at 298 K.

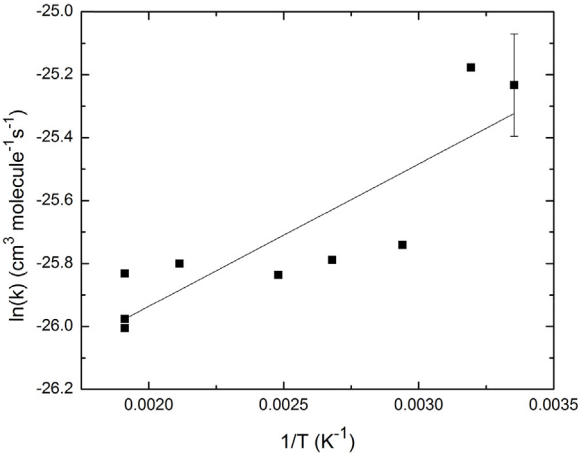

Figure 3. Arrhenius Plot of $\ln k$ (with k in cm^3 $molecule^{-1}$ s^{-1}) vs. $1/T$, for the $CN + CH_3Br$ reaction. Error bar represents one standard deviation.

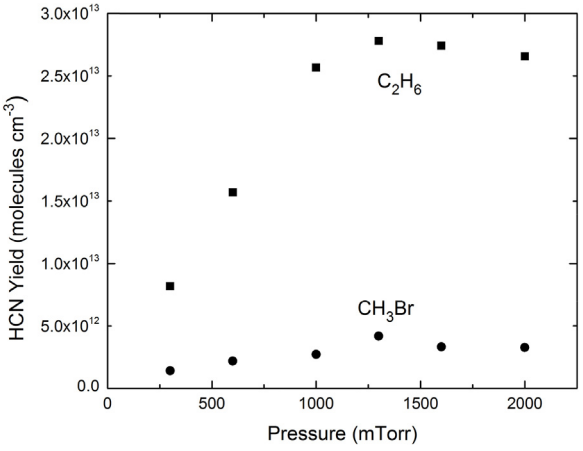

Figure 5. HCN yield as a function of CH_3Br (solid circles) and C_2H_6 (solid squares) reagent pressure. All data obtained at 298 K. P(ICN) = 0.1 Torr, P(SF_6) = 0.5 Torr, P(CH_3Br) = variable (lower trace only), P(C_2H_6) = variable (upper trace only).

abstraction reactions, and is in contrast to the positive activation energy previously reported for the $CN + CH_3Cl$ reaction [32], suggesting that a different mechanism may dominate. An Arrhenius fit to the data provides the following expression:

$$k_1(T) = (2.20 \pm 0.6) \times 10^{-12} \exp(453 \pm 98/T)\,\mathrm{cm^3\ molecule^{-1}\ s^{-1}}$$

where the error bars represent one standard deviation. This leads to an activation energy of $Ea = -3.76 \pm 0.8$ kJ mol^{-1}. At 298 K, the rate constant is $k_1 = (1.10 \pm 0.1) \times 10^{-11}$ cm^3 $molecule^{-1}$ s^{-1}.

3.2. Product yields

Infrared diode laser absorption spectroscopy was used to detect HCN products of the reactions of CN with CH_3Br. The $CN + C_2H_6$ reaction, which is expected to produce HCN in unity yield, was used as a reference reaction. Figure 4 shows typical transient signals. The peak amplitudes of these signals were converted into absolute number densities using linestrengths from the HITRAN database [35]. For the P(19) line at 3251.822 cm^{-1}, the linestrength is $S_{vj} = 8.31 \times 10^{-20}$ cm molecule^{-1}. Figure 5 shows the resulting HCN yield as a function of CH_3Br and C_2H_6 pressures. As shown, the HCN yield increases with increasing reagent (CH_3Br or C_2H_6) pressure up to a limiting value at which all of the photolytically

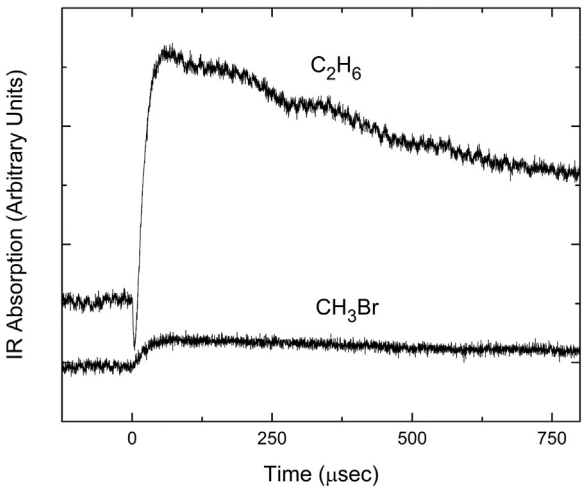

Figure 4. Transient infrared absorption signals for HCN product detection from the $CN + CH_3Br$ and $CN + C_2H_6$ reactions at 298 K. P(ICN) = 0.10 Torr, P(CH_3Br) = 1.6 Torr (lower trace only), P(C_2H_6) = 1.6 Torr (upper trace only), P(SF_6) = 0.5 Torr.

produced CN radicals have reacted with the reagent. At low reagent pressures, competing CN removal processes such as self reaction, diffusional decay, and reaction with trace oxygen result in lower HCN product yields. The key result of this experiment is that it demonstrates that the HCN yield of the $CN + CH_3Br$ is much lower than that of the $CN + C_2H_6$ reference reaction (which is assumed to produce HCN in unity yield). By comparing yields of HCN at pressures of CH_3Br or C_2H_6 of 1.0 Torr or greater, we estimate a branching fraction of only 0.12 ± 0.02 for channel (1a). This is in qualitative agreement with ab initio calculations [33] that suggested the possibility of alternate product channels such as (1b), (1c), or (1d). Most HCN yield experiments were performed at 298 K, but we did perform one experiment at an elevated temperature (473 K), obtaining identical results as those at 298 K.

Note that in the above discussion, the assignment of unity yield for HCN production in the $CN + C_2H_6$ reference reaction is an assumption, and has not been experimentally proven to our knowledge. We can, however, compare the HCN yields in this reaction to a rough estimate of the initial number of CN radicals created in our experiment, based on a previously measured 266-nm absorption coefficient of the ICN precursor ($\sim$0.009 cm^{-1} $Torr^{-1}$, base e) [34], assuming a unity quantum yield for CN production from ICN photolysis, and the measured pulse energies in this experiment. We typically find that the HCN yield is $\sim$70% of the estimated $[CN]_0$. Although the uncertainties in this estimate are substantial, it does demonstrate that HCN is at least the dominant channel of the reference reaction.

One issue that could affect the product yield results is the possibility that the reaction produces HCN with nascent vibrational or rotational excitation. The linestrengths in the HITRAN database that we use to convert transient signal amplitudes assumes a room temperature Boltzmann distribution of quantum states. Any rotational relaxation is expected to be quickly relaxed by collisions, and the use of SF6 buffer gas probably causes vibrational excitation to be also relaxed, but we are not aware of literature data that verifies this. Therefore, in order to test whether this is an issue, we performed some experiments in which we measured the static HCN absorption after firing multiple photolysis laser shots (typically 50), using our standard reaction mixtures. This approach is generally less accurate than using transient signals, because of possible secondary chemistry due to buildup of products, any secondary chemistry slower than the timescale of the transient signals, and possible wall reactions. Nevertheless, this approach allows any vibrational excitation to relax to a Boltzmann distribution. We find that the ratio of static HCN produced by 50 photolysis shots upon

an ICN/CH_3Br/SF_6 mixture is only 13% of that produced by an equal number of photolysis shots on an ICN/C_2H_6/SF_6 mixture, in almost perfect agreement with the transient signal results. Either the HCN is produced vibrationally cold, or the relaxation rates are sufficient high to relax any vibrationally excited HCN on the timescale ($\sim$50 μs) of the transient signals.

Products from channels (1b), (1c), and (1d) are in principle detectable, although with very low sensitivity. Using published spectroscopic data [41] we were able to locate several BrCN lines at 2202.523, 2203.025, and 2202.965 cm^{-1}. No transient signals at these locations were detected upon photolysis of ICN/SF_6/CH_3Br mixtures, but small static absorption lines at these wavelengths were observed to slowly appear over the course of $\sim$100 photolysis laser pulses. Observation of these same spectral lines using neat BrCN samples shows that these are extremely weak absorption lines, so the absence of transient signals does not allow us to draw any quantitative conclusions regarding the yield of BrCN. Nevertheless, it appears that BrCN is a product of reaction (1), possibly the major product. Similarly, CH_3CN products from channel (1c) can be detected near 2290 cm^{-1}. Again, spectral lines in this wavelength region are very weak based on observations using neat CH_3CN samples. No transient signals were observed, and only very small static absorption lines were observed over several hundred photolysis laser pulses. Based on this observation, we believe that channel (1c) is at most a minor product channel. Lastly, we searched for HBr product molecules at 2649.092 cm^{-1}. Again, no transient signals were observed. Furthermore, no static absorption lines were observed even after several hundred photolysis laser pulses. For this molecule, HITRAN linestrengths are available [37]; the line used has a linestrength of 4.46×10^{-20} cm molecule^{-1}. Based on this, we estimate an upper limit of $\sim$0.01 for the branching fraction of channel (1b).

4. Discussion

The primary experimental result in this study is the finding that hydrogen abstraction to form HCN + CH_2Br, channel (1a), is only a minor product channel, with an estimated branching fraction of 0.12 ± 0.02. It is useful to compare this result with recent ab initio calculations [33]. In those calculations, Farahani et al. predicted a free energy barrier of 4.9 kcal/mol and 5.0 kcal/mol for hydrogen abstraction and bromine abstraction, respectively. They also used conventional transition state theory to predict rate constants of 3.3×10^{-12} cm^3 $molecule^{-1}$ s^{-1}, and 2.25×10^{-12} cm^3 $molecule^{-1}$ s^{-1} for the hydrogen abstraction and bromine abstraction channels, respectively, at 298 K; this predicts a total rate constant of 5.55×10^{-12} cm^3 $molecule^{-1}$ s^{-1}, somewhat smaller than our experimental value of 1.10×10^{-11} cm^3 $molecule^{-1}$ s^{-1}, but still reasonable agreement. Their rate constants predict a branching fraction of 0.6 into the hydrogen abstraction channel, which is considerably larger than our value of 0.12. Furthermore, their barrier heights would imply a positive activation energy, in contrast to the experimental observations. It appears, based on the experimental data, that the ab initio calculations probably overestimated the barrier height for the bromine abstraction channel. Nevertheless, the calculations and experiments are in qualitative agreement that hydrogen abstraction is not the only accessible channel, and therefore may not dominate the reaction, in contrast to reactions of CN with saturated hydrocarbons

It is also useful to compare our results to previous results for the CN + CH_3Cl reaction [32]. In that study, a slightly slower rate constant of 9.03×10^{-12} cm^3 $molecule^{-1}$ s^{-1} at 298 K was observed, and positive 10.1 kJ/mol activation energy was observed. Although direct HCN detection was not performed in those experiments, the kinetic data was consistent with hydrogen abstraction to form HCN as a major, possibly dominant channel, in agreement with recent calculations [33]. We therefore conclude that CH_3Cl and CH_3Br react with CN by different mechanisms.

5. Conclusions

The reaction of CN with CH_3Br is moderately fast at room temperature with a total rate constant of $(1.10 \pm 0.1) \times 10^{-11}$ cm^3 $molecule^{-1}$ s^{-1}. This reaction displays a small negative activation energy, suggesting, in agreement with theoretical predictions, that direct hydrogen abstraction to form HCN is not the dominant channel. Direct detection and quantification of the HCN yield verifies this result, indicating that HCN formation accounts for only 12% of the reaction rate. The dominant channel was not quantified, but is most likely BrCN + CH_3.

Acknowledgement

This work was supported by the Division of Chemical Sciences, Office of Basic Energy Sciences of the Department of Energy, Grant DE-FG03-96ER14645.

References

[1] D.L. Baulch, C.J. Cobos, R.A. Cox, P. Frank, G. Hayman, Th Just, J.A. Kerr, T. Murrells, M.J. Pilling, J. Troe, R.W. Walker, J. Warnatz, J. Phys. Chem. Ref. Data 23 (1994) 847.
[2] C. Anastasi, D.U. Hancock, J. Chem. Soc., Faraday Trans. 2 (84) (1988) 9.
[3] D.A. Lichtin, M.C. Lin, Chem. Phys. 96 (1985) 473.
[4] R.J. Balla, K.H. Castleton, J. Phys. Chem. 95 (1991) 2344.
[5] I.R. Sims, J.-L. Queffelec, D. Travers, B.R. Row, L.B. Herbert, J. Karthauser, I.W.M. Smith, Chem. Phys. Lett. 211 (1993) 461.
[6] L. Herbert, I.W.M Smith, R.D. Spencer-Smith, Int. J. Chem. Kinet. 24 (1992) 791.
[7] D.L. Yang, T. Yu, M.C. Lin, C.F. Melius, Chem. Phys. 177 (1993) 271.
[8] B. Atakan, J. Wolfrum, Chem. Phys. Lett. 186 (1991) 547.
[9] L.R. Copeland, F. Mohammed, M. Zahedi, D.H. Volman, W.M. Jackson, J. Chem. Phys. 96 (1992) 5817.
[10] W.P. Hess, J.L. Durant, F.P. Tully Jr., J. Phys. Chem. 93 (1989) 6402.
[11] G. Saidani, Y. Kalugina, A. Gardez, L. Biennier, R. Georges, F. Lique, J. Chem. Phys. 138 (2013) 124308.
[12] M.T. Butterfield, T. Yu, M.C. Lin, Chem. Phys. 169 (1993) 129.
[13] A. Gardez, G. Saidani, L. Biennier, R. Georges, E. Hugo, V. Chandrasekaran, V. Roussel, B. Rowe, K. Reddy, E. Arunan, Int. J. Chem. Kinet. 44 (2012) 753.
[14] H. Reisler, M. Mangir, C. Wittig, Chem. Phys. 47 (1980) 49.
[15] M.Y. Louge, R.K. Hanson, Int. J. Chem. Kinet. 16 (1984) 231.
[16] I.R. Sims, J.-L. Queffelec, A. Defrance, C. Rebrion-Rowe, D. Travers, P. Bocherel, B.R. Rowe, I.W.M. Smith, J. Chem. Phys. 100 (1994) 4229.
[17] R.C. Jensen, D.B. Walton, R.D. Coombe, Ber. Bunsen-Ges. Phys. Chem. 169 (1990) 441.
[18] J.L. Durant, F.P. Tully Jr., Chem. Phys. Lett. 154 (1989) 568.
[19] B. Atakan, A. Jacobs, M. Wahl, R. Weller, J. Wolfrum, Chem. Phys. Lett. 154 (1989) 449.
[20] M. Burmeister, S.K. Gulati, K. Natarajan, K. Theilen, E. Mozzhukin, P. Roth, Symp. (Int.) Combust. (Proc.) 22 (1989) 1083.
[21] I.R. Sims, I.W.M. Smith, J. Chem. Soc., Faraday Trans. 89 (1993) 1.
[22] Y.Y. You, N.S. Wang, J. Chin. Chem. Soc. (Taipei) 40 (1993) 337.
[23] W. Tsang, J. Phys. Chem. Ref. Data 21 (1992) 753.
[24] K.T. Rim, J.F. Hershberger, J. Phys. Chem. 103 (1999) 3721.
[25] W. Feng, J.F. Hershberger, J. Phys. Chem. 113 (2009) 3523.
[26] J. Park, J.F. Hershberger, J. Chem. Phys. 99 (1993) 3488.
[27] J. Park, J.F. Hershberger, Chem. Phys. Lett. 295 (1998) 89.
[28] W. Feng, J.F. Hershberger, J. Phys. Chem. A. 115 (2011) 286.
[29] W. Feng, J.F. Hershberger, J. Phys. Chem. A 110 (2006) 12184.
[30] W. Feng, J.F. Hershberger, J. Phys. Chem. A 116 (2012) 10285.
[31] E. Janssen, J.F. Hershberger, Chem. Phys. Lett. 625 (2015) 26.
[32] V. Samant, J.F. Hershberger, Chem. Phys. Lett. 460 (2008) 64.
[33] P. Farahani, S. Maeda, J.S. Francisco, M. Lundberg, ChemPhysChem 16 (2015) 181.
[34] W.F. Cooper, J. Park, J.F. Hershberger, J. Phys. Chem. 97 (1993) 3283.
[35] H. Okabe, Photochemistry of Small Molecules, Wiley-Interscience, 1978.
[36] W.F. Cooper, J.F. Hershberger, J. Phys. Chem. 96 (1992) 771.
[37] L.S. Rothman, et al., J. Quant. Spectrosc. Radiat. Transfer 48 (1992) 469.
[38] A. Maki, W. Quapp, S. Klee, G.C. Mellau, S. Albert, J. Mol. Spectrosc. 10 (1996) 323.
[39] A.G. Maki, G.C. Mellau, S. Klee, M. Winneisser, W. Quapp, J. Mol. Spectrosc. 202 (2000) 67.
[40] D. Cerny, R. Bacis, G. Guelachvili, F. J. Rousx, Mol. Spectrosc. 73 (1978) 154.
[41] F. Tamassia, C. Degli Esposti, L. Dore, G. Cazzoli, J. Mol. Specrosc. 174 (1995) 59.